

The decay $\tau^- \rightarrow K^- K^+ \pi^- \nu_\tau$ and the ν_τ mass

J. J. Gomez-Cadenas

Santa Cruz Institute for Particle Physics, University of California, Santa Cruz, California 95064

M. C. Gonzalez-Garcia and A. Pich

Departamento de Fisica Teorica and Instituto de Fisica Corpuscular (Consejo Superior de Investigaciones Cientificas), Universidad de Valencia, 46100 Burjasot, Spain

(Received 5 April 1990)

In this paper, we present a model based on the effective chiral Lagrangian to describe the decay $\tau^- \rightarrow K^- K^+ \pi^- \nu_\tau$. Using our model we study the possible limits on the ν_τ mass that can be achieved by a high-statistics, high-precision experiment taking data close to the τ -pair production threshold.

I. INTRODUCTION

The possibility of a nonzero neutrino mass is obviously a very important question in particle physics. There is no fundamental principle requiring a null mass for the neutrino. On the contrary, many extensions of the standard model predict nonvanishing neutrino masses, which could have, in addition, important implications in cosmology and astrophysics.

The ν_τ , unlike its two closest relatives, the ν_e and ν_μ , has not yet been directly observed. The best tool that we have at present to extract information about this particle is provided by the study of τ decays.

The current limit on the mass of the ν_τ ,¹

$$m_{\nu_\tau} < 35 \text{ MeV, } 95\% \text{ C.L.}, \quad (1.1)$$

is much worse than the limits on the electron-neutrino mass,² $m_{\nu_e} < 18 \text{ eV}$, and the muon-neutrino mass,³ $m_{\nu_\mu} < 250 \text{ keV}$. Note, however, that in many extensions of the standard model a mass hierarchy among different generations is expected, with the neutrino mass being proportional to some power of the mass of its charged-lepton partner. Assuming for instance the fashionable relation⁴ $m_{\nu_\tau}/m_{\nu_e} \sim (m_\tau/m_e)^2$, the bound (1.1) would be equivalent to a limit of 3 eV in the mass of the electron neutrino. A relatively crude measurement of m_{ν_τ} may imply then strong constraints on neutrino-mass model building.

The limit (1.1) could be very much improved by an experiment running at the recently proposed^{5,6} “ τ -charm” factory, a new low-energy ($E_{\text{c.m.}} \sim 3\text{--}4.5 \text{ GeV}$), high-luminosity ($10^{33} \text{ cm}^{-2}\text{s}^{-1}$) e^+e^- collider. With the planned integrated luminosity of $15 \text{ fb}^{-1} \text{ yr}^{-1}$, typical yearly rates of 10^7 τ pairs could be produced.

The possibility of reducing the m_{ν_τ} upper bound in a future τ -charm factory has been already considered. It has been shown^{7,8} that the study of the decay $\tau \rightarrow e \bar{\nu}_e \nu_\tau$ could result in a limit of the order of 20–30 MeV, thus providing little improvement of the current limit. More promising looks the study of the end point of the

hadronic-mass spectrum of high-multiplicity hadronic τ decays to high-hadronic-mass final states, such as the decays $\tau^- \rightarrow K^- K^+ \pi^- \nu_\tau$ and $\tau^- \rightarrow \pi^- \pi^+ \pi^- \pi^+ \pi^- \nu_\tau$ (references in this paper to a specific charge state are to be understood as implying also the conjugate state). The possible limits that can be achieved by studying the decay $\tau^- \rightarrow \pi^- \pi^+ \pi^- \pi^+ \pi^- \nu_\tau$ have been analyzed recently.⁹ Assuming that this decay mode proceeds through the chain $\tau^- \rightarrow \rho^0 \rho^0 \pi^- \nu_\tau$ with $\rho^0 \rightarrow \pi^+ \pi^-$, it has been estimated⁹ that a sensitivity on m_{ν_τ} of the order of 3.5 MeV (which corresponds to 30 fb^{-1} of data) could be achieved by an experiment studying this decay in the τ -charm factory. However, there is a large uncertainty in this limit associated with the unknown underlying dynamics of the hadronic final state, which could modify drastically the expectation of the naive model used. Although the shape of the hadronic-mass spectrum near the end point is obviously not sensitive to the details of the hadronic dynamics, the particular resonance structure of the final hadrons governs the fraction of events occurring near the end point of the distribution, and therefore, the estimate of the possible sensitivity, achievable in a future experiment, does depend on the assumed hadronic model.

In this paper we analyze the prospects for improving the m_{ν_τ} upper bound through the study of the decay mode $\tau^- \rightarrow K^- K^+ \pi^- \nu_\tau$. At present, the limit extracted from the study of this channel,¹⁰ $m_{\nu_\tau} < 157 \text{ MeV}$ (95% C.L.), is rather poor compared with the bound (1.1) obtained from the $\tau^- \rightarrow \pi^- \pi^+ \pi^- \pi^+ \pi^- \nu_\tau$ decay. This is mainly due to the limited statistics collected in the $\tau^- \rightarrow K^- K^+ \pi^- \nu_\tau$ mode. When future large τ -decay data samples are available, this channel could become competitive because, first, its branching fraction is not too low [$B_{\tau^- \rightarrow K^- K^+ \pi^- \nu_\tau} = (0.22^{+0.17}_{-0.11})\%$], and, second, it peaks at rather big values of hadronic invariant mass, in spite of its moderate multiplicity. On the other hand, this low multiplicity makes it easier to handle theoretically the strong dynamics of the final state.

The theoretical study of the $\tau^- \rightarrow K^- K^+ \pi^- \nu_\tau$ decay is done in Sec. II, using a dynamical model which incorpo-

rates the chiral-symmetry constraints of QCD and the resonance structures present in this channel. In Sec. III we discuss the experimental aspects such as event selection and background suppression, while in Sec. IV we discuss the projected sensitivity to m_{ν_τ} . Finally, in Sec. V we present our conclusions.

II. THE DECAY $\tau^- \rightarrow K^- K^+ \pi^- \nu_\tau$

At low momentum transfer, the coupling of a state H of n pseudoscalars to the $V - A$ current can be estimated in a very easy way by using the effective chiral realization of QCD, which, to lowest order in derivatives and masses, is given by¹¹

$$L_{\text{strong}} \approx \frac{1}{4} f_\pi^2 \text{Tr}(\partial_\mu U \partial^\mu U^\dagger) + \nu \text{Tr}(MU + U^\dagger M). \quad (2.1)$$

The 3×3 special unitary matrix $U = \exp(i\sqrt{2}\Phi/f_\pi)$ incorporates the octet of pseudoscalar mesons, which appear as Goldstone coordinate fields $\phi(x)$,

$$\Phi(x) = \frac{\lambda}{\sqrt{2}} \phi(x) = \begin{pmatrix} \frac{\pi^0}{\sqrt{2}} + \frac{\eta}{\sqrt{6}} & \pi^+ & K^+ \\ \pi^- & -\frac{\pi^0}{\sqrt{2}} + \frac{\eta}{\sqrt{6}} & K^0 \\ K^- & \bar{K}^0 & -\frac{2\eta}{\sqrt{6}} \end{pmatrix}, \quad (2.2)$$

M denotes the diagonal quark mass matrix, $M = \text{diag}(m_u, m_d, m_s)$, and

$$\nu = \frac{f_\pi m_{\pi^+}^2}{2(m_u + m_d)} = \frac{f_\pi^2 m_{K^+}^2}{2(m_u + m_s)} = \frac{f_\pi^2 m_{K^0}^2}{2(m_d + m_s)}. \quad (2.3)$$

In this realization, the vector and axial-vector currents are given by¹²

$$V_\mu = i(\Phi \vec{\partial}_\mu \Phi) + O(\Phi^4) - \frac{iN_c}{6\sqrt{2}\pi^2 f_\pi^3} \epsilon_{\mu\nu\alpha\beta} [\partial^\nu \Phi \partial^\alpha \Phi \partial^\beta \Phi + O(\Phi^5)], \quad (2.4)$$

$$A_\mu = \sqrt{2} f_\pi \partial_\mu \Phi - \frac{\sqrt{2}}{3f_\pi} [\Phi, (\Phi \vec{\partial}_\mu \Phi)] + O(\Phi^5) - \frac{N_c}{12\pi^2 f_\pi^4} \epsilon_{\mu\nu\alpha\beta} [\partial^\nu \Phi \partial^\alpha \Phi (\Phi \vec{\partial}^\beta \Phi) + O(\Phi^6)], \quad (2.5)$$

where the odd-parity pieces, proportional to the Levi-Civita pseudotensor, come from the Wess-Zumino-Witten term of the chiral Lagrangian¹³ which takes into account the non-Abelian chiral anomaly of QCD.

Tau decays involve, however, high values of momentum transfer, where the formulas given above no longer apply. Nevertheless we can still construct a reasonable

model, taking into account the low-energy theorems contained in the chiral realization. The amplitudes

$$T_\mu(P_1, \dots, P_n) = \left\langle H \left| (V - A)_\mu \exp \left[i \int d^4z L_{\text{strong}}(z) \right] \right| 0 \right\rangle \quad (2.6)$$

obtained from Eqs. (2.1)–(2.5) must be continued from threshold by suitable final-state-interaction enhancements, which take into account the possible resonance structures present in each channel in a phenomenological way.^{12,14,15} This can be done by weighting the contribution of a given set of pseudoscalars with definite quantum numbers, with the appropriate resonance form factor. The requirement that the chiral predictions must be recovered below the resonance region fixes the normalization of these form factors to be one at zero invariant mass. We take the standard ansatz

$$F_R(s) = \frac{M_R^2}{M_R^2 - s - iM_R \Gamma_R(s)}, \quad (2.7)$$

where M_R (Γ_R) denotes the mass (width) of the resonance R .

Let us now apply this model to the decay $\tau^- \rightarrow K^- K^+ \pi^- \nu_\tau$. The decay amplitude can be written as

$$M = \frac{G_F}{\sqrt{2}} \cos \theta_C \bar{u}_\nu \gamma^\mu (1 - \gamma_5) u_\tau T_\mu, \quad (2.8)$$

with u_τ and u_ν being the spinors of the τ and ν_τ , respectively, θ_C the Cabibbo angle, and $T_\mu = T_\mu(P_{K^-}, P_{K^+}, P_{\pi^-})$ the hadronic matrix element.

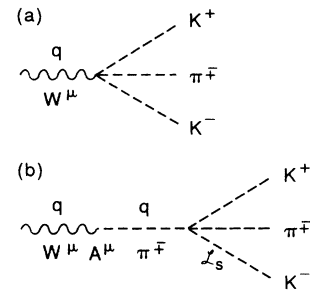


FIG. 1. Diagrams contributing to the hadronic amplitude T_μ . (a) represents the contribution coming directly from the piece with three mesons of the hadronic current corresponding to the normal axial-vector current plus anomalous vector current. (b) represents the contribution coming from the piece of the axial-vector current with only one pseudoscalar combined with a strong vector.

At lowest order in the effective-chiral-Lagrangian theory there are two different diagrams contributing to the hadronic amplitude T_μ . The first contribution, Fig. 1(a), comes directly from the piece with three mesons of the hadronic current corresponding to the normal axial-vector current plus the anomalous vector current. The second contribution, Fig. 1(b), comes from the piece of the axial-vector current with only one pseudoscalar, combined with a strong vertex. The matrix element can be written as

$$T_\mu = T_\mu^{1^-} + T_\mu^{1^+},$$

where the index 1^+ (1^-) is used to label the axial-vector (vector) piece. Neglecting corrections of order $m_\pi^2/q^2 \sim m_\pi^2/m_\tau^2$, one finds

$$T_{1^+}^\mu = \frac{\sqrt{2}i}{3f_\pi} \left[g^{\mu\nu} - \frac{q^\mu q^\nu}{q^2} \right] [(P_{K^+} - P_{K^-})_\nu F_{1^-}(s) + (P_{K^+} - P_{\pi^-})_\nu F_{1^-}(t)] F_{1^+}(q^2),$$

$$T_{1^-}^\mu = \frac{\sqrt{2}}{4f_\pi^3 \pi^2} \epsilon^{\mu\nu\alpha\beta} P_{K^- \nu} P_{K^+ \alpha} P_{\pi^- \beta} F_{1^-}(s) F_{1^-}(t) F_{1^-}(q^2),$$

where we have introduced the kinematical variables

$$\begin{aligned} u &= (q - P_{K^+})^2 = (P_{K^-} + P_{\pi^-})^2, \\ t &= (q - P_{K^-})^2 = (P_{K^+} + P_{\pi^-})^2, \\ s &= (q - P_{\pi^-})^2 = (P_{K^+} + P_{K^-})^2. \end{aligned} \quad (2.11)$$

The $F_{1^-}(q^2)$ form factor could be obtained, in principle, from the isovector part of the $e^+e^- \rightarrow K\bar{K}\pi$ cross section; unfortunately, the large isoscalar contribution to this process makes the extraction of the isovector amplitude rather problematic with the present data.¹⁶

Using SU(3) symmetry, $F_{1^-}(q^2)$ can also be obtained from the $e^+e^- \rightarrow \eta\pi^+\pi^-$ cross section.^{15,17} Taking the values¹⁸ $M_{\rho'} = 1590$ MeV and $\Gamma_{\rho'} = \Gamma_{\rho'}(M_{\rho'}^2) = 260$ MeV, the invariant-mass distribution of the $\eta\pi^+\pi^-$ final state can be reasonably well described with a combination of ρ and ρ' resonances:

$$F_{1^-}(q^2) = [F_{\rho'}(q^2) + \xi F_{\rho}(q^2)] / (1 + \xi), \quad (2.12)$$

with a mixing parameter $\xi = -4$. Since the $e^+e^- \rightarrow \eta\pi^+\pi^-$ data^{19,20} have large errors, we will also consider the extreme values $\xi = -3.5$ and $\xi = -4.5$, which provide an overestimate and an underestimate, respectively, of the $\eta\pi^+\pi^-$ production cross section.

It has been recently claimed^{19,21} that the $\rho'(1600)$ structure may actually consist of two overlapping resonances ρ' and ρ'' . Unfortunately, the data are rather inconclusive. To see how the presence of an additional resonance near the end point could affect the sensitivity of this decay channel to the ν_τ mass, we have also fitted the $e^+e^- \rightarrow \eta\pi^+\pi^-$ data with a combination of ρ , ρ' , and ρ'' resonances:

$$T_\mu^{1^-} = \frac{\sqrt{2}}{4f_\pi^3 \pi^2} \epsilon_{\mu\nu\alpha\beta} P_{K^- \nu} P_{K^+ \alpha} P_{\pi^- \beta}, \quad (2.9)$$

$$T_\mu^{1^+} = \frac{\sqrt{2}i}{3f_\pi} \left[g_{\mu\nu} - \frac{q_\mu q_\nu}{q^2} \right] (2P_{K^+}^\nu - P_{K^-}^\nu - P_{\pi^-}^\nu),$$

where q^μ is the momentum transfer, $q^\mu = p^\mu - p'^\mu = P_{K^+}^\mu + P_{K^-}^\mu + P_{\pi^-}^\mu$ and therefore q^2 is the squared invariant mass of the $KK\pi$ system.

Equations (2.9) are valid only at low values of q^2 ; nevertheless, they fix the normalization of the hadronic amplitudes. These low-energy results should be modulated with the possible two-body ($K^+\pi^-$, K^+K^-) and three-body ($K^+K^-\pi^-$) resonance form factors. Taking that into account, the $J^P=1^+$ and $J^P=1^-$ amplitudes can be parametrized as

$$F_{1^-}(q^2) = \frac{F_{\rho''}(q^2) + \epsilon F_{\rho'}(q^2) + \delta F_{\rho}(q^2)}{1 + \epsilon + \delta}. \quad (2.13)$$

A reasonable fit is obtained with $M_{\rho'} = 1500$ MeV, $\Gamma_{\rho'} = 220$ MeV, $M_{\rho''} = 1750$ MeV, $\Gamma_{\rho''} = 120$ MeV, $\epsilon = 6.5$, and $\delta = -26$. These masses and widths are in fair agreement with those obtained in Ref. 19. To take into account experimental uncertainties, we will allow the parameter δ to vary between $\delta = -25$ and $\delta = -27$.

Both fits to the $e^+e^- \rightarrow \eta\pi^+\pi^-$ data have been done using $F_{1^-}(s) = 1$ and $F_{1^-}(t) = F_{\rho}(t)$, i.e., taking into account the two-body resonance $\rho(\pi^+\pi^-)$. Since we are assuming SU(3) symmetry, we will use the same form factors in the τ decay amplitude of Eq. (2.10).

The axial amplitude can be directly taken from the $\tau^- \rightarrow \nu_\tau \pi^+ \pi^- \pi^-$ decay mode, which is mediated by the resonance A_1 . Using here $F_{1^-}(s) = F_{\rho}(s)$, $F_{1^-}(t) = F_{\rho}(t)$, and $F_{1^+}(q^2) = F_{A_1}(q^2)$, a good description of the existing data is obtained¹² with the resonance parameters $M_{A_1} = 1200$ MeV and $\Gamma_{A_1} = \Gamma_{A_1}(M_{A_1}^2) = 475$ MeV.

Once the hadronic input is given, it is straightforward to compute the $\tau^- \rightarrow K^- K^+ \pi^- \nu_\tau$ decay width. The q^2 distribution can be written as

$$\begin{aligned} \frac{d\Gamma}{dq^2} &= \frac{G_F^2 \cos^2 \theta_C}{384(2\pi)^5 m_\tau^3} \bar{\omega}(q^2, m_\tau^2, m_{\nu_\tau}^2) \lambda^{1/2}(m_\tau^2, q^2, m_{\nu_\tau}^2) \\ &\quad \times [I_{1^+}(q^2) + I_{1^-}(q^2)], \end{aligned} \quad (2.14)$$

where $\bar{\omega}$ is the so-called ‘‘weak matrix element’’

$$\begin{aligned} \bar{\omega}(q^2, m_\tau^2, m_{\nu_\tau}^2) &= (m_\tau^2 - q^2)(m_\tau^2 + 2q^2) \\ &\quad - m_{\nu_\tau}^2(2m_\tau^2 - q^2 - m_{\nu_\tau}^2) \end{aligned} \quad (2.15)$$

and the kinematical function $\lambda^{1/2}(m_\tau^2, q^2, m_{\nu_\tau}^2)$ is defined by

$$\begin{aligned} \lambda^{1/2}(m_\tau^2, q^2, m_{\nu_\tau}^2) &= (\{m_\tau^2 - [(q^2)^{1/2} + m_{\nu_\tau}]^2\} \\ &\quad \times \{m_\tau^2 - [(q^2)^{1/2} - m_{\nu_\tau}]^2\})^{1/2} \\ &= 2m_\tau |\mathbf{P}_{\nu_\tau}|. \end{aligned} \quad (2.16)$$

The functions I_{1+} and I_{1-} are the hadronic-phase-space integrals

$$\begin{aligned} I_{1+}(q^2) &= \frac{-1}{(q^2)^2} \int ds dt T_{1+}^\mu T_{1+\mu}, \\ I_{1-}(q^2) &= \frac{-1}{(q^2)^2} \int ds dt T_{1-}^\mu T_{1-\mu}. \end{aligned} \quad (2.17)$$

In Fig. 2, we show the predicted hadronic-mass distribution. The solid curve corresponds to the case where only one ρ' resonance is considered (with $\xi' = -4$), while the dashed curve is the behavior obtained in the ρ' - ρ'' scenario (with $\delta' = -26$.) Note that, although in the second case the distribution peaks at lower values of q^2 , due to the dominance of the $\rho'(1500)$ enhancement, the presence of the additional $\rho''(1750)$ resonance produces a small increase in the population near the end point.

The decay width turns out to be completely dominated by the 1^- amplitude (the contribution of the axial-vector channel amounts to less than 10% of the total width). The predicted branching ratio, together with the fraction of events near the end point of the distribution [$(q^2)^{1/2} > 1750$ MeV], f_{end} , is given in Table I, for the different hadronic assumptions considered. These results are consistent with the present experimental value¹⁰ of $(0.22^{+0.17}_{-0.11})\%$.

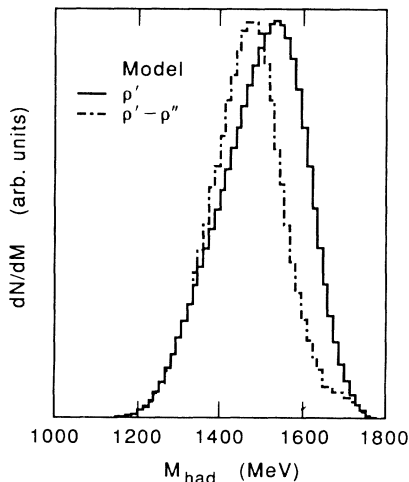


FIG. 2. Predicted hadronic-mass distribution. The solid line is for the model with only one ρ' resonance ($\xi' = -4$), while the dashed line corresponds to the model with a ρ', ρ'' combination ($\delta' = -26$).

TABLE I. Model predictions.

Model	Parameters	B (%)	f_{end}
$\rho'(1590)$	$\xi = -3.5$	0.35	6.5×10^{-4}
	$\xi = -4$	0.26	5.9×10^{-4}
	$\xi = -4.5$	0.21	5.2×10^{-4}
$\rho'(1500)$	$\delta = -25$	0.38	8.3×10^{-4}
	$\delta = -26$	0.34	8.1×10^{-4}
$\rho''(1750)$	$\delta = -27$	0.29	7.8×10^{-4}

III. THE τ -CHARM-FACTORY EXPERIMENT FOR MEASURING m_{ν_τ}

A. The τ -charm detector

To study the limits on m_{ν_τ} that can be achieved in an experiment running at a τ -charm factory, we have made a simulation of this experiment. A preliminary design of the proposed accelerator has been given in Ref. 22 and further work is discussed in Ref. 6. The detector design has also been extensively discussed in Ref. 6. Here, we will only outline its main features. The detector is a very compact 4π detector, able to track particles in 95% of the solid angle with a state-of-the-art low-mass drift chamber, and with electromagnetic and hadronic calorimetry covering 99% of the solid angle. Particle identification is achieved through the combination of electromagnetic and hadronic calorimetry, muon range and time-of-flight (TOF) and dE/dx measurements. Since the average particle momentum in a τ -charm factory experiment is low ($P < 1$ GeV) these techniques are very effective. Our global rejection factor to separate electrons (muons) from hadrons is of the order of 10^{-3} (10^{-2}).

The most relevant detector for the study of the ν_τ mass is the drift chamber. It is designed as a cylindrical volume of radius 100 cm and length 360 cm operating in a moderate magnetic field of 0.6 T. The inner wall is contiguous with the beam pipe to allow a vertex constrained fit which will improve the measurement of the track angles. The drift-chamber gas must be light, to minimize multiple scattering. This can be accomplished by using helium-rich mixtures (for the simulation of the detector we presently use a mixture of 72% helium, 15% carbon dioxide, and 7% isobutane at a pressure of 1 atm). The design momentum resolution is

$$\left(\frac{\sigma_p}{p} \right)^2 = [0.4\% p \text{ (GeV)}]^2 + (0.3\% / \beta)^2.$$

For our study we have used a full simulation of the detector (see Ref. 6) that includes the effect of multiple Coulomb scattering and energy loss in the beam pipe and in the chamber material as well as the detector inefficiencies, cracks, etc. Our τ generator incorporates our model for the decay $\tau^- \rightarrow K^- K^+ \pi^- \nu_\tau$. For the

simulation of the hadronic background we have used the Lund Monte Carlo²³ model.

In this paper we will assume the design parameters of the τ -charm machine, peak luminosity of $10^{33} \text{ cm}^{-2} \text{ s}^{-1}$ and one year of physics run of 274 days, yielding an integrated luminosity of $15 \text{ fb}^{-1} \text{ yr}^{-1}$.

B. Event selection and background suppression

The optimum energy to perform an experiment to measure the ν_τ mass is at $\sqrt{s}=3.68 \text{ GeV}$, close to the τ production-cross-section peak but still below the production threshold for c and b quarks, thus avoiding a potentially serious source of background. The background due to the light quarks u, d, s can be understood in detail by taking data below the τ production threshold. Furthermore, at $\sqrt{s}=3.68 \text{ GeV}$, the topology of the multihadronic background events tend to be very spherical, and therefore their invariant mass tend to peak close to the center-of-mass energy, while the signal events tend to peak at the τ mass. This fact by itself provides a suppression of the background of the order of 10^2 as can be clearly seen in Fig. 3.

The event selection is based on “tagging” one τ and imposing the other one to decay via $\tau^- \rightarrow K^- K^+ \pi^- \nu_\tau$. For tagging we will take advantage that the lepton spectrum (electrons and muons) of the multihadronic background is peaked at low energies (since the leptons in the background are due essentially to decays and gamma and Dalitz conversions), and the missing energy is very close to zero (since there are no emitted neutrinos) except in events where energy escapes in the forward direction or a neutral hadron (n, K_L^0) fails to be detected by the hadronic calorimeter. Consequently, imposing events with a high-energy lepton, significant transverse momentum, and large missing energy will reduce drastically the background. On the other hand, the τ leptonic decays

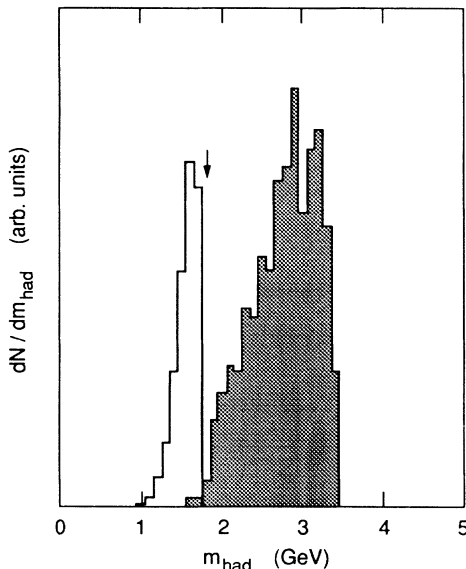


FIG. 3. Hadronic mass for the signal and the hadronic background (shaded). The arrow marks the τ mass.

$\tau \rightarrow e \bar{\nu}_e \nu_\tau$ and $\tau \rightarrow \mu \bar{\nu}_\mu \nu_\tau$ have a lepton spectrum that peaks at relatively high energy, and large missing energy and transverse momentum due to the two undetected neutrinos. Since the neutrino emitted by the tau decaying via $\tau^- \rightarrow K^- K^+ \pi^- \nu_\tau$ is carrying very little momentum, all the missing energy and momentum in the event is due to the τ decaying via $\tau \rightarrow l \bar{\nu}_l \nu_\tau$. Therefore, we will tag our events imposing the following: (1) a lepton of energy bigger than 400 MeV; no other leptons in the event; (2) missing transverse momentum bigger than 200 meV; (3) missing energy bigger than 800 MeV. In Fig. 4 we illustrate our selection criteria. The arrows mark the selection cuts.

To guarantee good momentum measurement and particle identification we will limit production angles to $|\cos\theta| < 0.9$, where θ is the track polar angle. Neither electromagnetic nor hadronic neutral energy must be detected in the calorimeters (the energy deposited in the electromagnetic calorimeter must be less than 30 MeV;

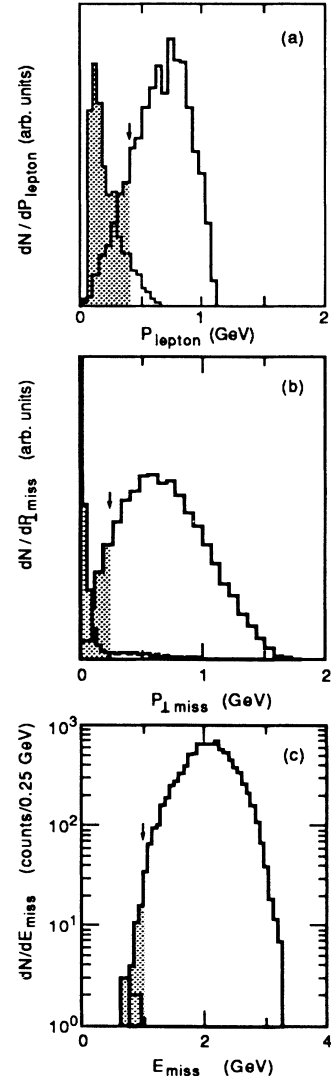


FIG. 4. (a) Lepton spectrum, (b) missing transverse momentum, and (c) missing energy after cuts (a) and (b) for the signal and the background (shaded).

the energy deposited in the hadronic calorimeter must be less than 50 MeV). Events where any of the tracks are observed to decay in the drift chamber are also thrown away. Our global efficiency is about 20%. The main reasons why we lose signal events are the strict requirements for tracking and the decays in the drift chamber of any of the produced hadrons. On the other hand, our selection criteria will provide a very efficient suppression of the background. The only relevant background to our process are multihadronic events of the type

$$e^+e^- \rightarrow \gamma \rightarrow u, d, s, \rightarrow 4 \text{ charged tracks.}$$

Before the cuts, the ratio R of signal to potential background is

$$R = \frac{\sigma_{\tau^+\tau^-} B_{\tau^- \rightarrow K^- K^+ \pi^- \nu_\tau} 2B_{\tau^- \rightarrow l \bar{\nu}_l \nu_\tau}}{\sigma_{\text{had}} B_c}.$$

Here, B_c is defined as the branching fraction of multihadronic events with four charged tracks (and any number of neutrals) in the final state, $B_c \approx 40\%$. Since $\sigma_{\tau^+\tau^-}/\sigma_{\text{had}} \approx 0.15$ we find $R = 5.4 \times 10^{-4}$. However, the rejection due only to the “lepton + E_{miss} ” cut is 10^5 . After tagging, with no further conditions $R = 50$. The requirement of not having neutral energy detected and exactly two-kaons and one pion provides an additional rejection of 10^2 . Therefore, $R \sim 5 \times 10^3$. But still, the condition that the hadronic mass of the system has to be less than the τ mass will provide an additional rejection of at least 10^2 . Consequently we find that, if the τ -charm projected detector requirements (excellent time of flight, hermetic, compact detector, very good hadronic calorimetry) are met, we can obtain an essentially background-free data sample.

IV. LIMITS ON m_{ν_τ}

Once the events have passed the selection criteria, we compute the invariant mass of the hadronic system. As discussed above, because of the low momentum of the hadrons emitted, the momentum resolution and thus, the mass resolution, is very good. With the projected drift chamber described in the preceding section, the mass resolution is 2 MeV. The effect of the multiple scattering of the hadrons in the beam pipe is found to be negligible in comparison with the multiple scattering of the hadrons in the drift chamber, which is the dominant cause of the mass resolution.

The limits that can be achieved on the τ neutrino mass, $\delta(m_{\nu_\tau})$, depend on the mass resolution and on the data sample that can be achieved:

$$\delta(m_{\nu_\tau}) \propto \frac{\delta(m_{\text{had}})}{\sqrt{N_{\text{end point}}}},$$

where $\delta(m_{\text{had}})$ is the hadronic-mass resolution and $N_{\text{end point}}$ is the number of events with hadronic mass bigger than 1750 MeV (per unit time):

$$N_{\text{end point}} \sim 2N_{\tau^+\tau^-} [B(\tau \rightarrow e \bar{\nu}_e \nu_\tau) + B(\tau \rightarrow \mu \bar{\nu}_\mu \nu_\tau)] \\ \times B(\tau^- \rightarrow K^- K^+ \pi^- \nu_\tau) \epsilon f_{\text{end}}.$$

Here, the number of τ pairs produced per unit time is $N_{\tau^+\tau^-}$ (3.6×10^7 per year); the efficiency to detect the signal is $\epsilon = 20\%$; the branching fraction for the “tag” τ is taken $B(\tau \rightarrow e \bar{\nu}_e \nu_\tau) = B(\tau \rightarrow \mu \bar{\nu}_\mu \nu_\tau) = 18\%$, $B(\tau^- \rightarrow K^- K^+ \pi^- \nu_\tau)$ is the branching fraction for the decay $\tau^- \rightarrow K^- K^+ \pi^- \nu_\tau$ and f_{end} the fraction of events near the end point of the hadronic-mass distribution ($m_{\text{had}} > 1750$ MeV).

The technique to determine m_{ν_τ} is to compare the hadronic-mass distribution with the functional form predicted by the theory. This function is obtained from Eq. (2.14) as

$$\frac{d\Gamma}{dm_{\text{had}}} \propto m_{\text{had}} \bar{\omega}(m_{\text{had}}^2, m_\tau^2, m_{\nu_\tau}^2) \lambda^{1/2}(m_\tau^2, m_{\text{had}}^2, m_{\nu_\tau}^2) \\ \times [I_{1+}(m_{\text{had}}^2) + I_{1-}(m_{\text{had}}^2)]. \quad (4.1)$$

To estimate the sensitivity that can be achieved on the τ neutrino mass, we have generated decays $\tau^- \rightarrow K^- K^+ \pi^- \nu_\tau$ assuming different neutrino masses ($m_{\nu_\tau} = 1, 5, 10,$ and 20 MeV) and performed a χ^2 minimization fit to the corresponding distributions. We have fit the end point of the hadronic-mass distribution ($m_{\text{had}} > 1750$ MeV) to Eq. (4.1) folded with a resolution function describing the detector mass resolution. A more detailed discussion of this technique can be found in Ref. 9.

In Table II we show the limits that can be achieved on m_{ν_τ} (at 95% C.L.) as a function of the parameters of our model. We assume that the τ -charm factory will be able to collect at least 30 fb^{-1} of data for this experiment (see Ref. 6).

As it can be seen, the most pessimistic extreme of the model predicts a factor-2 improvement over the present limit. The ρ' - ρ'' scenario provides a better limit of the order of 10 MeV, improving the current limit in more than a factor of 3. This sensitivity is still poor, when compared with the expected one for the decay channel $\tau^- \rightarrow \pi^- \pi^+ \pi^- \pi^+ \pi^- \nu_\tau$, $\delta(m_{\nu_\tau}) \sim 3.5$ MeV⁹. Note, however, that our better theoretical understanding of the $\tau^- \rightarrow K^- K^+ \pi^- \nu_\tau$ decay mode makes it a very useful

TABLE II. Limits on m_{ν_τ} (30 fb^{-1} data set).

Model	Parameters	$\delta(m_{\nu_\tau})$ (in MeV at 95% C.L.)
$\rho'(1590)$	$\xi = -3.5$	11.6
	$\xi = -4.0$	14.2
	$\xi = -4.5$	16.8
$\rho'(1500)$ +	$\delta = -25$	9.9
	$\delta = -26$	10.6
$\rho''(1750)$	$\delta = -27$	11.7

cross check of the study of the decay $\tau^- \rightarrow \pi^- \pi^+ \pi^- \pi^+ \pi^- \nu_\tau$ which will probably have the dominant sensitivity to the τ neutrino mass.

V. SUMMARY

We have considered the possibility of improving the ν_τ mass limit by studying the decay $\tau^- \rightarrow K^- K^+ \pi^- \nu_\tau$ in an experiment running at the proposed τ -charm factory. We have developed a model to describe the decay $\tau^- \rightarrow K^- K^+ \pi^- \nu_\tau$, which incorporates the chiral-symmetry constraints of QCD and the available information of the relevant resonance structures. Our model agrees well with present data. For a given scenario (the ρ' - ρ'' case), we find that with the projected luminosity and detector capabilities the present limit can be reduced by more than a factor 3, reaching an ultimate limit of the

order of 10 MeV. A slightly weaker bound of about 20 MeV is obtained if only one ρ' is assumed.

ACKNOWLEDGMENTS

We are indebted to both A. De Rújula and J. Kirkby for pointing us the interest of this analysis. We are also thankful to C. A. Heusch and A. Seiden for useful discussions. M.C.G-G. wants to acknowledge the hospitality of the Santa Cruz Institute for Particle Physics and SLAC theory group during the time in which this work was realized. The work of two of us (M.C.G-G. and A.P.) has been partially supported by CICYT, Spain, under Grant No. AEN 89-0348. Finally, J.J.G-C. wants to acknowledge the support of a Fulbright Grant during part of the time of this work. This work was supported in part by the U.S. Department of Energy contract No. DE-AC03-765-ff00515.

¹ARGUS Collaboration, H. Albrecht *et al.*, Phys. Lett. B **202**, 149 (1988).

²M. Fritschi *et al.*, Phys. Lett. B **173**, 485 (1986).

³R. Abela *et al.*, Phys. Lett. **146B**, 431 (1984).

⁴M. Gell-Mann, P. Ramond, and R. Slansky, in *Supergravity*, edited by D. Z. Freedman and P. van Nieuwenhuizen (North-Holland, Amsterdam, 1979), p. 315.

⁵J. Kirkby, CERN Report No. CERN-EP/87-210, 1987 (unpublished); J. Kirkby, Particle World **1**, 27 (1989).

⁶See *Proceedings of the τ -Charm Factory Workshop*, Stanford, California, 1989, edited by Lydia V. Beers (SLAC Report No. 343, Stanford, 1989).

⁷J. J. Gomez-Cadenas and M. C. Gonzalez-Garcia, Phys. Rev. D **39**, 1370 (1989).

⁸R. R. Mendel *et al.*, Z. Phys. C **32**, 517 (1986).

⁹J. J. Gomez-Cadenas *et al.*, Phys. Rev. D **41**, 2179 (1990).

¹⁰DELCO Collaboration, G. B. Mills *et al.*, Phys. Rev. Lett. **54**, 624 (1985).

¹¹See, for example, H. Georgi, *Weak Interactions and Modern Particle Theory* (Benjamin/Cummings, Menlo Park, California, 1984.)

¹²A. Pich, in *Proceedings of the τ -Charm Factory Workshop*

(Ref. 6), p. 416.

¹³J. Wess and B. Zumino, Phys. Lett. **37B**, 95 (1971); E. Witten, Nucl. Phys. **B223**, 422 (1983).

¹⁴R. Fischer, J. Wess, and F. Wagner, Z. Phys. C **3**, 313 (1980).

¹⁵A. Pich, Phys. Lett. B **196**, 561 (1987).

¹⁶DM1 Collaboration, F. Mane *et al.*, Phys. Lett. **112B**, 178 (1982).

¹⁷F. J. Gilman, Phys. Rev. D **35**, 3541 (1987).

¹⁸Particle Data Group, M. Aguilar-Benitez *et al.*, Phys. Lett. **170B**, 1 (1986).

¹⁹DM2 Collaboration, A. Antonelli *et al.*, Phys. Lett. B **212**, 133 (1988).

²⁰VEPP-2M Collaboration, V. P. Drughinin *et al.*, Phys. Lett. B **174**, 115 (1986); DM1 Collaboration, B. Delcourt *et al.*, Phys. Lett. **113B**, 93 (1982).

²¹A. Donnachie and H. Mirzaie, Z. Phys. C **33**, 407 (1987); A. Donnachie and A. B. Clegg, *ibid.* **34**, 257 (1987); S. Fuki *et al.*, Phys. Lett. B **202**, 441 (1988).

²²J. Jowett, Reports Nos. CERN-LEP-TH/87-56, 1987 (unpublished) and CERN-LEP-TH/88-22, 1989 (unpublished).

²³T. Sjostrand and M. Bengtsson, Comput. Phys. Commun. **43**, 367 (1987).

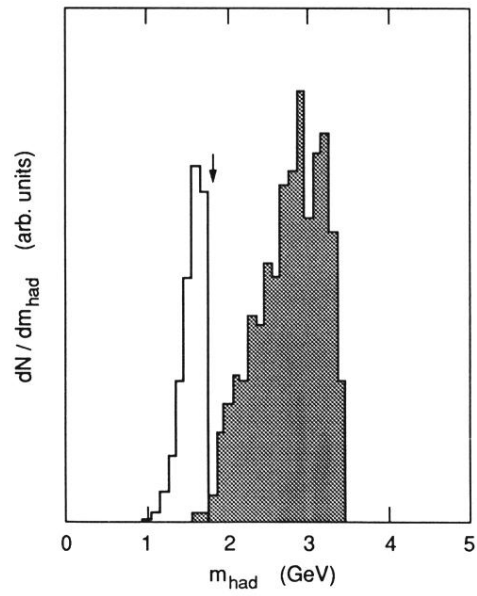


FIG. 3. Hadronic mass for the signal and the hadronic background (shaded). The arrow marks the τ mass.

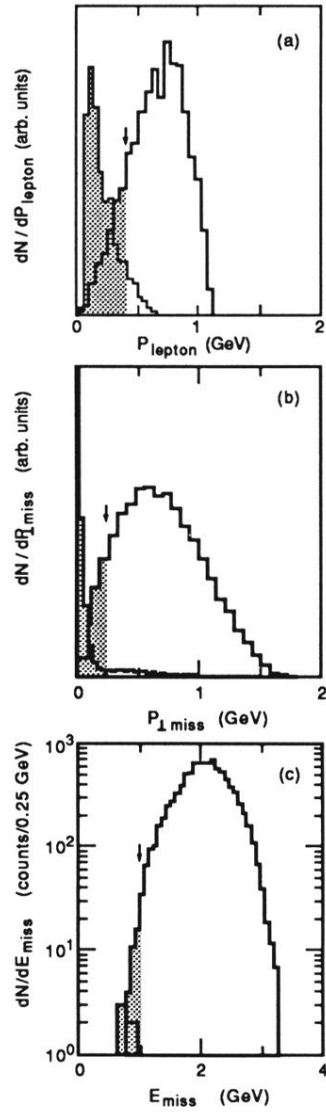


FIG. 4. (a) Lepton spectrum, (b) missing transverse momentum, and (c) missing energy after cuts (a) and (b) for the signal and the background (shaded).